中国激光

高重复频率极紫外光源的产生和光谱技术研究进展

王佶[1,2]，赵昆[1,2*]

[1]中国科学院物理研究所，北京凝聚态物理国家研究中心，北京 100190；

[2]松山湖材料实验室，广东 东莞 523808

摘要 高重复频率极紫外光源已被广泛应用于电子动力学研究，并且在阿秒谱学研究和显微成像中有广阔的应用前景。高重复频率极紫外光源正在朝更高重复频率、更高光子通量、更高光子能量和更短脉宽的方向发展。介绍了高重复频率极紫外光源的产生和调控，以及极紫外光源应用的分辨能力优化，并展望了高重复频率极紫外光源的未来发展趋势。

关键词 非线性光学；超快光学；高次谐波；极紫外光源

中图分类号 O437 **文献标志码** A **DOI**：10.3788/CJL231498

1 引 言

自1987年人们首次发现高次谐波辐射以来[1-2]，极紫外高次谐波光源由于其相干性强[3]、脉冲短、光子能量高等特点，在电子动力学研究领域中受到了广泛关注[4-7]。极紫外光源被广泛应用于各类谱学和成像研究中。人们对电子运动过程的探索催生了时间分辨-角分辨光电子能谱技术，利用高重复频率、高光子通量的窄线宽飞秒（1 fs=10^{-15} s）极紫外光源，可以实现材料导带结构和飞秒尺度下电子动力学特性的直接观察。进一步地，科学家们对阿秒（1 as=10^{-18} s）尺度下超快动力学演化过程的探索则催生了阿秒瞬态吸收光谱。使用100电子伏特（eV）以下的宽谱阿秒光源，人们已经对电子隧穿、分子解离等过程进行了深入探索[8-10]。利用近几年发展的水窗波段宽光谱阿秒光源[11-14]，可以进一步探测分子间的反应路径[13]及材料表面的载流子运动[15]等重要的微观化学和物理过程。除直接探测光谱外，借助电子和离子探测手段，可以实现时间分辨符合谱学测量等阿秒瞬态谱学研究[16]。对于阿秒时间尺度上的电子谱学测量，单发测量的事件数往往不够，使得低重复频率光源不足以获得可信的统计数据，因此需要使用高重复频率的极紫外阿秒光源。在超快谱学飞速发展的同时，人们也在追求更高分辨率的显微成像技术。X射线相干衍射成像常使用重复频率为几十赫兹（Hz）到1千赫兹的窄线宽极紫外光源，利用衍射图样对微纳结构乃至纳米液滴进行显微成像[17-19]。低光子通量的光源在有限的曝光时间内会降低显微成像的信噪比，因此也有人尝试使用高重复频率的极紫外光源进行实时显微成像[20]。近年来还有实验成功使用宽带极紫外光源进行了相干衍射成像，未来有望实现阿秒时间分辨、纳米空间分辨的高精度成像[21]。

角分辨光电子能谱（ARPES）实验在研究材料的电子结构方面具有独特的动量分辨能力，是极紫外光源的主要测量手段之一[22]。在ARPES实验中，材料中的电子首先被深紫外或极紫外光子电离，然后被电子分析器收集。在过去的十年里，超快激光和传统ARPES技术的巨大进步，以及非平衡电子结构研究的热潮，刺激了时间分辨ARPES（Tr-ARPES）的发展[23-26]。Tr-ARPES结合了ARPES和超快激光技术，其中使用的光源包括两束超短脉冲。一束是近红外脉冲，作为泵浦脉冲将样品激发到非平衡态。另一束是探测电子结构的极紫外脉冲。这两个超快脉冲在时域上是相干的，它们的时间延迟可以通过两脉冲的光程差进行调节。

Tr-ARPES中使用的近红外-深紫外光源可以基于非线性光学效应产生，例如光学晶体中的非线性效应[23]。这一方法可以较为容易地产生深紫外脉冲，并且可以通过调节色散实现高能量和时间分辨率。然而，使用这种方法产生的探测脉冲光子能量通常小于7 eV，导致布里渊区的测量范围通常小于0.81 Å^{-1}，不足以测量布里渊区边界附近的电子结构，例如过渡金属二硫族化物或石墨烯。为了实现更大的布里渊区测量范围，人们设计了基于高次谐波的光源。高次谐波产生的极紫外光源可以用来研究在大动量位置含有关

收稿日期：2023-12-11；**修回日期**：2024-01-17；**录用日期**：2024-02-05；**网络首发日期**：2024-02-20

基金项目：国家自然科学基金（92150103，61690221）、中国科学院稳定支持基础研究领域青年团队计划（YSBR-059）

通信作者：*zhaokun@iphy.ac.cn

键电子结构的材料[27]。此外，通过使用单色仪可以进一步实现可调谐的极紫外(XUV)光源。光子-电子散射的截面和极紫外脉冲穿透材料的深度强烈依赖于光子能量，因此一些电子态可以利用一定能量范围内的光子获得，可调谐XUV光源在Tr-ARPES实验中发挥着重要作用[28]。

本文将首先回顾高重复频率驱动激光和高重复频率高次谐波的产生方法，之后讨论如何实现极紫外光的光谱筛选和测量以及极紫外束线的分辨率优化。最后，还将探讨极紫外光源的其他应用，并展望未来高重复频率极紫外光源的发展趋势。

2 高次谐波的驱动激光

高次谐波的产生可以用半经典的三步模型进行描述[29]。当一束强激光脉冲照射到气体原子上时，原子中的基态电子会通过隧穿电离被激光脉冲激发到连续态。为了达到隧穿电离所需的电场强度，驱动激光的功率密度需要为10^{13}～10^{15} W/cm^2[30]。电离后，初速为零的电子波包在激光场中被加速，并有可能最终回到母核附近。最后，电子和母核复合回到基态，其电子动能和原子电离能转化为光子动能，产生光谱在极紫外至软X射线波段的高次谐波辐射。驱动激光脉冲产生的高次谐波脉冲在频域上表现为梳齿状分立的光谱，每个梳齿中心对应的光子能量通常为驱动激光光子能量的奇数倍。在时域上，一个高次谐波脉冲包含等间隔的阿秒脉冲序列，称为阿秒脉冲串，其间隔为驱动激光脉冲的半个光周期。

由于极紫外高次谐波的分立光谱特性，通过挑选出单阶次的高次谐波，可进一步得到窄线宽的飞秒量级极紫外光源。目前，可应用于Tr-ARPES的窄线宽极紫外光源主要朝更高通量、更高重复频率的方向发展，这对飞秒激光器的重复频率和单脉冲能量提出了较高要求。自1985年啁啾脉冲放大(CPA)技术[31]问世以来，钛宝石激光的峰值功率得到了极大提升[32]。目前，脉冲宽度小于30 fs的钛宝石激光器被广泛应用于高次谐波及孤立阿秒脉冲产生实验[33]。钛宝石激光器的单脉冲能量可以达到1 mJ以上，适于获得高光子能量和产生更短的孤立阿秒脉冲，但其重复频率通常仅为1～10 kHz[34]。近些年人们也对高重复频率钛宝石激光系统的搭建及高重复频率极紫外光源的产生展开了研究。Chiang等[35]使用长腔型钛宝石激光器将驱动激光的重复频率提升到4 MHz，并得到了高次谐波输出。此外，也有使用重复频率为50～100 kHz的钛宝石激光器产生高次谐波的报道[36]。

相较于钛宝石激光器，光纤激光器具有更好的散热性，并且集成度高，因此更适合作为高平均功率、高重复频率的驱动源[37-41]。2014年，Rothhardt等[42]使用光纤激光器，结合相干合成，得到了重复频率为150 kHz的水窗波段极紫外光源。同年Hädrich等[43]使用光纤激光器，结合四路相干合成，使用重复频率为600 kHz、脉冲能量为150 μJ、脉冲宽度为29 fs的驱动光，获得了光通量达3×10^{13} photon/s的高次谐波光源。次年他们进一步将驱动激光的重复频率提升至10.7 MHz[44]。2016年，Müller等[45]使用八路相干合成获得了平均功率超过1 kW的激光输出。而目前飞秒激光器的最高平均功率已经达到了10 kW以上[46]。在2019年以前，人们在Tr-ARPES应用中普遍使用钛宝石激光器产生高次谐波，其重复频率低于10 kHz[47-52]，而Tr-ARPES束线的能量分辨率只能达到150 meV。Puppin等[53]首次在2019年使用重复频率为500 kHz的基于掺镱光纤激光器的光参量啁啾放大(OPCPA)光源，获得了能量分辨率为121 meV、光子通量为2×10^{11} photon/s(在样品处测量光子通量，下同)的单级高次谐波光源。此后高重复频率的高次谐波被广泛应用于Tr-ARPES。同年，Mills等[54]使用重复频率为60 MHz、单脉冲能量为200 nJ的掺镱光纤激光器，借助飞秒增强腔(fsEC)，得到了能量分辨率为22 meV、光子通量为10^{11} photon/s的单级高次谐波光源。2023年，Csizmadia等[55]使用重复频率为100 kHz、脉冲宽度为6 fs的光纤激光器，得到了能量分辨率为120 meV的光谱可调谐准单色高次谐波光源。同年，Wang等[56]使用重复频率为400 kHz、压缩后脉冲宽度为25 fs的光纤激光光源，获得了能量分辨率为96 meV的光谱可调谐准单色高次谐波光源，其光子通量达到2×10^{12} photon/s。

高功率光纤激光器的复杂程度高，而且受放大自发辐射(ASE)的影响，产生的脉冲基座会降低主脉冲的峰值功率[33]。而以掺镱固体材料为基础的全固态激光器则能够使用较为简单的结构获得足够高的峰值功率，全固态激光是继光纤激光之后的理想的高重复频率驱动激光[57]。2015年，Emaury等[58]使用重复频率为2.4 MHz的薄片振荡器，将脉冲宽度从870 fs非线性压缩至108 fs以产生高次谐波，得到了光子通量为5×10^7 photon/s的极紫外光，首次实现了使用飞秒振荡器直接产生高次谐波[33]。2014年，Lorek等[57]使用全固态商业激光器，在100 kHz重复频率下实现了光子通量为4.4×10^{10} photon/s的高次谐波输出。2020年Yb全固态激光器开始应用于Tr-ARPES束线，Liu等[59]使用重复频率为150 kHz、脉冲宽度为280 fs、单脉冲能量为133 μJ的基于掺镱钨酸钆钾晶体(Yb∶KGW)放大器的固体激光器，得到了能量分辨率为21.5 meV、光子通量为2.5×10^8 photon/s的单阶高次谐波光源。Cucini等[60]使用重复频率为200 kHz、脉宽为250 fs的OPCPA光源，将能量分辨率提升至19 meV。Lee等[61]使用基于Yb∶KGW的重复频率为250 kHz、脉宽为190 fs的激光器，通过其三倍频驱动获得九次谐波，进一步将单阶极紫外光的能量分辨率提升至16 meV。

2022 年，Guo 等[62]使用重复频率为 250 kHz、脉冲宽度为 461 fs 的基于掺镱钇铝石榴石（Yb:YAG）的全固态激光器，获得了能量分辨率为 9～18 meV 的高次谐波，这是目前极紫外飞秒光源驱动 Tr-ARPES 的最佳能量分辨率。高重复频率极紫外光源的发展离不开高重复频率、高平均功率超强激光的发展[63]，以碟片振荡器为基础的全固态激光器和高功率光纤激光器是未来的主要发展方向。

而对于需要宽光谱、短脉宽极紫外阿秒光源的阿秒瞬态光谱学应用，则需要利用载波包络相位（CEP）稳定的少周期激光产生高次谐波和阿秒脉冲并作为瞬态吸收光谱的泵浦光。为了得到高重复频率且 CEP 稳定的少周期激光，需要高重复频率振荡器及增益带宽大且对 CEP 影响小的放大器。光参量放大由于其放大过程几乎不影响 CEP 的稳定性，且放大过程中的热效应较低，因此适用于高重复频率且 CEP 稳定的激光放大器。但单级光参量放大的带宽较窄，难以支持少周期脉冲的放大，需要使用两级或多级光参量放大，针对不同光谱成分进行分别放大，达到输出少周期飞秒激光的目的。目前，基于高重复频率驱动源的极紫外阿秒脉冲产生已有多次报道。2013 年，Krebs 等[64]使用少周期钛宝石种子源和两级 OPCPA 光源，得到了重复频率为 600 kHz、脉冲宽度为 6.6 fs、CEP 稳定的驱动激光，并进一步获得了 XUV 超连续谱，对应的单个阿秒脉冲宽度为 338 as。2017 年，Furch 等[65-66]使用两级 OPCPA 的 CEP 稳定的脉冲宽度为 7 fs 的光源，在 100 kHz 重复频率下获得了脉冲宽度为 160 as 的孤立阿秒脉冲，之后他们又将结果提升至 130 as 左右，光子通量达到了 10^6 photon/pulse[67]。2018 年，Harth 等[68]使用钛宝石振荡器，经过两级 OPCPA 后得到重复频率为 200 kHz、脉冲宽度为 6.1 fs、CEP 稳定的驱动激光，获得了少阿秒脉冲序列[69]，并将其进一步用于研究氦原子的电离[70]。Mikaelsson 等[16]利用这条高重复频率极紫外阿秒束线，配合三维电子/离子谱仪，实现了首个全角度分辨的氦原子单光子双电离符合测量。目前的百 kHz 高重复频率驱动激光已经达到了单脉冲能量为 1 mJ、脉宽为 7 fs、CEP 稳定的指标，未来将向更高的单脉冲能量方向发展[71]。

3 高次谐波通量的优化

极紫外光源的应用，如 ARPES 测量，需要一束极紫外光照射样品。样品表面的电子被极紫外光激发至连续态，光电子动能和发射角度则包含样品的能带结构信息。带有角度分辨功能的电子分析器接收到辐射出的这些光电子，从而得到样品价带附近的能带结构。对于低重复频率的极紫外光源，由于其单发脉冲含有大量的光子，故会在短时间内在样品表面激发出大量光电子。库仑相互作用将带来严重的光电子动能分布展宽，称为空间电荷效应。为减小空间电荷效应的影响，需要在维持光子通量不变的情况下，减小每一发脉冲所含的光电子，因此需要高重复频率的驱动激光产生高重复频率的极紫外光源。高重复频率高次谐波的产生效率和光通量均难以与低重复频率高次谐波比拟[72-73]。高重复频率驱动激光的单脉冲能量较低，所以需要通过紧聚焦才能获得产生高次谐波的场强[74]。而紧聚焦时激光和气体的作用区域很小，达到所需的相位匹配条件也相对困难，因此高重复频率高次谐波的转换效率很低[72]。为了提高高重复频率高次谐波的光子通量，人们采取了各种改进方法。部分具有代表性可用于 Tr-ARPES 的高次谐波光源，其通量及产生方法如表 1 所示，其中 SHG 表示二倍频，THG 表示三倍频。

增加通量最直接的方法是优化高重复频率高次谐波产生的相位匹配条件[75]和电离条件[76]。高次谐波的相位失配[75]主要由以下三项构成：由 Gouy 相位引起的聚焦导致的几何失配（Δk_{Gouy}），原子和自由电子引入的色散（$\Delta k_{\mathrm{Dispersion}}$）和强度依赖的偶极相位引入的失配项（$\Delta k_{\mathrm{Dipole}}$）[77-79]。在高次谐波产生实验中，通常需要通过调节作用区域的气压，实现相位匹配条件。焦点中心处的相位匹配气压[36]可表示为

$$p=\frac{p_0\lambda^2}{2\pi^2\omega_0^2\Delta\delta\left(1-\eta/\eta_c\right)},\tag{1}$$

式中：p 为相位匹配气压；λ 为驱动光波长；ω_0 为焦点处的光斑半径；p_0 为标准大气压；$\Delta\delta$ 为基频光和高次谐波的折射率差；η 为电离分数；η_c 为等离子体色散超过原子色散时的临界电离分数。当中心波长为 820 nm 时，相位匹配气压随焦点半径的变化如图 1[75] 所示。

可以看出，随着焦点半径的减小，相位匹配所需的气压增大。高重复频率高次谐波产生由于驱动激光的脉冲能量相对较低，需要使用紧聚焦获得足够的峰值功率密度，故相位匹配气压比一般的高次谐波产生要高。高气压对束线的真空环境产生了不利影响，同时高重复频率驱动激光的热效应也对气体靶带来了挑战。Puppin 等[53,56,62]使用气体喷嘴和集气口应对驱动激光的高功率并维持真空环境；Cucini 等[60]设计了气体喷嘴和隔离腔；Ojeda 等[50,80]使用带有水冷结构的气室（gas cell）结构，利用全铜结构实现散热和真空差分。

对于 Tr-ARPES 应用，减小驱动光波长、提高气体电离概率是获得高通量高次谐波的有效手段[76]。在单通高重复频率高次谐波产生过程中，基本都采取倍频或三倍频方法增加高次谐波的产生效率[53,56,59-60,62]。借助脉冲后压缩手段，使用更短脉冲的高重复频率驱动光可以更容易达到高次谐波产生所需的峰值功率密度，因此可以获得比长脉冲驱动更高的产生效率。

表 1 典型高次谐波光源的通量汇总

Table 1 Summary of fluxes of typical high-harmonic light sources

Ref.	Pulse energy of driving laser	Pulse duration /fs	Repetition rate /kHz	Photon flux at sample	Scheme for higher conversion efficiency	Gas target type
[52]	4000 μJ @ 800 nm	50	1	5.5×10^{10} photon/s @central photon energy of 26.4 eV	Focusing with focal length of 500 mm	
[47]	1000 μJ @ 780 nm	30	1	1.6×10^{10} photon/s @ central photon energy of 32.5 eV	Focusing with focal length of 250 mm	
[50]	1000 μJ @ 800 nm	45	6	2.3×10^{11} photon/s @ central photon energy of 36.3 eV	Focusing with focal length of 400 mm	
[48]	2800 μJ @ 785 nm	40	10	6×10^{8} photon/s @ central photon energy of 32.6 eV	Focusing with focal length of 600 mm	
[49]	300 μJ @ 390 nm	25	10	1×10^{9} photon/s @ central photon energy of 22.1 eV	SHG and waveguide	
[55]	1000 μJ @ 1030 nm	6	100	2.8×10^{10} photon/s @ central photon energy of 34.9 eV	Focusing with focal length of 900 mm	Water cooled gas cell
[59]	67 μJ @ 513 nm	280	150	2.5×10^{8} photon/s @ central photon energy of 21.8 eV	SHG + tight focusing	Gas cell
[60]	29 μJ @ 515 nm	290	200	6×10^{9} photon/s @ central photon energy of 16.9 eV	SHG + tight focusing	Gas jet + separation chamber
[62]	88 μJ @ 343 nm	461	250	7×10^{8} photon/s @ central photon energy of 25.3 eV	THG + annular beam + tight focusing	Gas jet + counter nozzle
[56]	12 μJ @ 515 nm	25	400	2×10^{12} photon/s @ central photon energy of 21.6 eV	Post compression+two-color field+tight focusing	Gas jet + counter nozzle
[53]	10 μJ @ 330 nm	40	500	2×10^{11} photon/s @ central photon energy of 21.7 eV	OPCPA + SHG	Gas jet + counter nozzle
[54]	0.33 μJ @ 1045 nm	120	60000	$>10^{11}$ photon/s @ central photon energy of 25 eV	fsEC	Gas jet

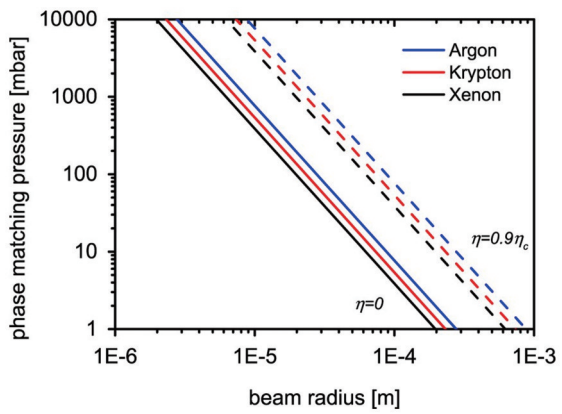

图 1 驱动光波长为 820 nm 时第 17 阶高次谐波对应的相位匹配气压[75]

Fig. 1 Phase matching pressure corresponding to 17th order high harmonic when wavelength of driving light is 820 nm[75]

Wang 等[56]使用双色场配合脉冲后压缩得到了目前 Tr-ARPES 样品测量的最高光子通量。使用大能量、少周期的高性能高重复频率激光器可以避免紧聚焦，从而可利用基频驱动光来获得较高的高次谐波产生效率[55]。重复频率在 MHz 以上的单通高次谐波产生，需要激光器的平均功率非常高，而一般的高重复频率激光器难以达到单通高次谐波产生所需的单脉冲能量，故重复频率在 MHz 以上的高重复频率高次谐波光源需要使用场增强的方式产生。目前具有代表性的场增强技术为基于纳米结构的等离子体增强和共振增强腔[81-82]。其中，共振增强腔已实际应用于 Tr-ARPES 束线。Mills 等[54]使用重复频率为 60 MHz 的光纤激光，借助共振增强腔，在光子通量达到 10^{11} photon/s 的同时，单发脉冲所包含的光子数不到 2000。而对于阿秒谱学测量所需的高重复频率极紫外阿秒光源，需要使用长波长的驱动激光产生单阿秒脉冲，因此通常使用高单脉冲能量、少周期的驱动激光确保获得足够的高次谐波光子通量[67]。

4 单色仪和光谱仪设计

极紫外高次谐波光源应用于实验时不能缺少单色仪或光谱仪。为了调节相互作用配置以优化高次谐波，以及使用阿秒瞬态吸收光谱等对能级跃迁进行表征，需要具有高采集效率且高分辨率的光谱仪[10]。而在动力学研究的泵浦-探测实验中，需要能量分辨和时间分辨能力都较好的飞秒极紫外光源，故需要设计单色仪挑选单个阶次的高次谐波，实现能量分辨的控制并减小单色仪带来的时间展宽。光子能量可调的极紫外光源可以在样品的竖直波矢方向上覆盖一个至多个布里渊区，将 ARPES 等原本的二维能带测量扩展到

三维[83]。对于这类应用，还需要单色仪具有光子能量可调谐的功能。

窄线宽的极紫外光源有助于ARPES实验获得高能量分辨率，进而实现对精细能带结构的测量。目前能量分辨率最高的ARPES束线，其分辨率接近1 meV[84]。能量分辨率为1～10 meV的ARPES束线能够实现对能带细节及能级改变和移动的准确测量，为材料学研究的诸多问题如观测过渡金属二硫族化物中电子空穴“口袋”的演化[85]、拓扑相转变[86-87]、电荷密度波（CDW）材料中掺杂对态密度的影响[83]等提供帮助。而这类高能量分辨的极紫外光源目前还只能通过气体灯或同步辐射等直接获得。

以高能量分辨率为特点的静态ARPES可以用来研究价带顶附近的能带结构及外界条件如温度等对其的影响。而为了研究导带的能带结构及电子动力学特性，需要借助有时间分辨特性的ARPES。Tr-ARPES在ARPES的基础上加入了泵浦-探测模块。实验中极紫外光源作为探测光，用于激发材料表面的光电子。还需要另一束飞秒激光作为泵浦光，用于将材料价带中的电子激发到导带。与静态ARPES所需的高单色性光源不同，Tr-ARPES的极紫外泵浦光和飞秒探测光都是脉冲宽度在飞秒尺度的超短脉冲。因此，Tr-ARPES所使用的极紫外光源很难达到静态ARPES光源的高单色性。目前，Tr-ARPES束线达到的最高能量分辨率为16 meV，其对应的时间分辨率为250 fs[61]。Tr-ARPES在时间分辨和能量分辨平衡的参数配置下可以使用特殊设计的单色仪，而高能量分辨的参数配置一般仍依赖于高次谐波的光源线宽。相干衍射成像等成像学应用通常也需要将极紫外光源单色化，需要选出单阶高次谐波并聚焦到样品上，之后收集样品的衍射图样，反演获得样品信息[20]。

目前进行极紫外光源单色化的常用方案有两种：基于光栅的单色仪[47-48,50,52,54-56,60-61]和基于金属膜或多层膜反射镜的光谱滤波[49,51,53,59,62]。其中，基于平面光栅的单色仪一般为XCT（X-ray Czerny-Turner）结构[56,88-89]，即使用轮胎镜将极紫外光准直，经光栅分光后用第二块轮胎镜将其聚焦到出射狭缝上以选出单色光。也有使用单轮胎镜、单块凹面光栅、单块轮胎面光栅聚焦的设计[48,89-90]。单色仪可以较为高效地挑选出单色性好的极紫外光，并保留了宽范围的光子能量调谐性能，但同时也会引入脉冲前倾，造成时间展宽。单色仪也可以通过特殊设计减小甚至消除光栅带来的时间展宽[47,55-56]。使用金属膜或多层膜反射镜可以挑选出单阶高次谐波，并且几乎不会引入时间展宽，但其无法进一步减小极紫外光的线宽，其线宽通常依赖于产生的高次谐波源本身的线宽，光子能量调谐能力较为受限[49,51,53,59,62]。

阿秒瞬态吸收光谱这类宽光谱应用终端也对系统的时间分辨率和能量分辨率提出了较高要求[13,15]。阿秒瞬态吸收光谱利用极紫外阿秒脉冲使处于原子或分子基态的电子跃迁到激发态或电离态，利用红外激光脉冲实现激发态和激发态间或激发态和电离态之间的耦合，通过检测极紫外光谱的变化分析出多个电子态的超快动力学演化过程。阿秒瞬态吸收光谱执行的是全光谱测量，需要极紫外光源具有宽光谱，其时间分辨率可以达到百阿秒量级。同时，对跃迁能级的精细测量要求光谱仪能够对极紫外全光谱进行高分辨率测量，从而能够实时、准确地进行动力学表征。极紫外光谱仪通常使用罗兰圆光谱仪或平场光栅光谱仪[91-92]。在罗兰圆中，一块凹面匀刻线光栅通过分光将不同波长的光分布于罗兰圆上[93]，使用时需要移动探测器以扫描全部光谱范围[92]，故通常只用于光源的快速筛选。平场光栅光谱仪是最常见的用于光谱表征及测试的极紫外光谱仪，其结构为一块凹面变刻线光栅或一块轮胎镜/凹面镜和一块平面变刻线光栅的组合[91,94]。平场光栅光谱仪可以实现宽范围光谱的同时测量，其分辨率通常取决于光栅刻线数、光谱宽度和探测器配置。

5 能量分辨和时间分辨分析

在研究电子动力学问题时，更高的时间分辨率有助于追踪更快的事件。但对于Tr-ARPES等需要测量能带的泵浦探测实验来说，捕捉事件的前提是有足够高的能量分辨率，通常Tr-ARPES的能量分辨率为100 meV，时间分辨率为100 fs量级[47-56,59-62,95]。Tr-ARPES的能量分辨率（ΔE）取决于XUV的谱线宽度（ΔE_{XUV}）、空间电荷效应造成的能量展宽（ΔE_{SC}）和ARPES分析器的能量分辨率（$\Delta E_{\mathrm{ARPES}}$）[59]：

$$\Delta E=\sqrt{\Delta E_{\mathrm{XUV}}^2+\Delta E_{\mathrm{SC}}^2+\Delta E_{\mathrm{ARPES}}^2}。\tag{2}$$

其中$\Delta E_{\mathrm{ARPES}}$通常小于10 meV，远小于$\Delta E_{\mathrm{XUV}}$[59,62]。使用单色仪进行XUV的单色化时，单色仪输出的XUV线宽[96-97]可以表示为

$$\Delta\lambda_{\mathrm{c}}=\frac{\cos\beta}{(m\sigma_{\mathrm{c}}p)\Delta s},\tag{3}$$

$$\Delta\lambda_{\mathrm{o}}=\frac{\cos\mu}{m\sigma_{\mathrm{o}}p}\Delta s\approx\frac{1}{m\sigma_{\mathrm{o}}p}\Delta s,\tag{4}$$

式中：$\Delta\lambda_{\mathrm{c}}$和$\Delta\lambda_{\mathrm{o}}$分别为常规衍射安装（CDM）和离面安装（OPM）光栅单色仪的输出线宽；β为CDM光栅的衍射角；μ为OPM光栅的圆锥入射角；m为衍射阶次；σ_{c}和σ_{o}分别为CDM和OPM光栅的刻线密度；p为出射臂长；Δs为出射狭缝处的光斑尺寸。CDM和OPM光栅示意图如图2[96]所示。

Grazioli等[98]测量得到臂长为1.2 m的单色仪在出口狭缝处的XUV光斑大小约为120 μm。Ojeda等[50]反演出XUV光源大小为57～139 μm，单色仪的能量分辨率实际受XUV焦点大小的影响。泵浦探测实验

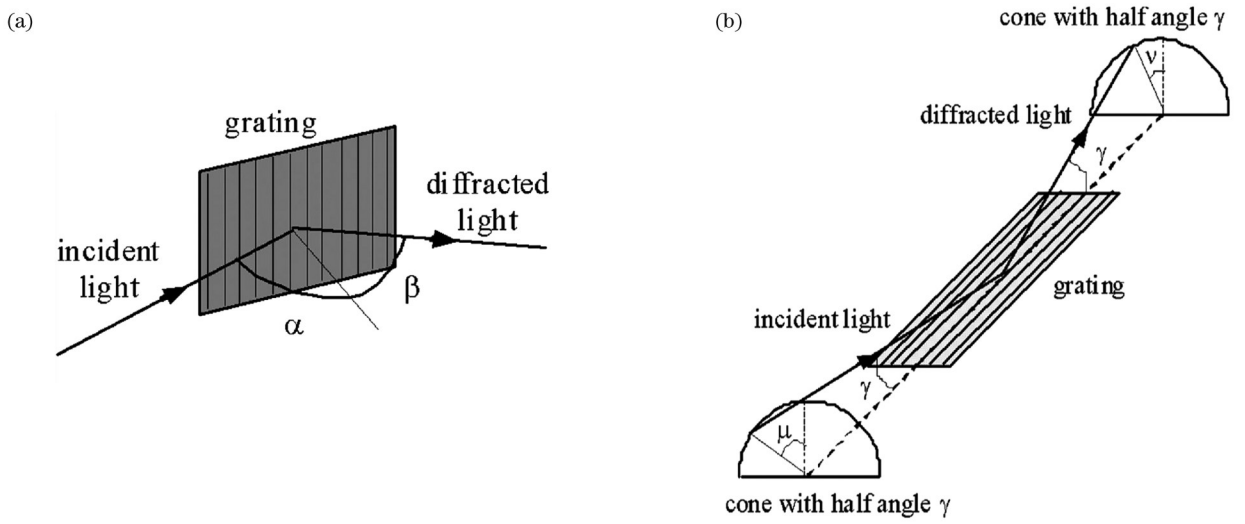

图 2　光栅安装示意图[96]。(a)CDM;(b)OPM

Fig. 2　Schematics of grating installation[96]. (a) CDM; (b) OPM

的时间分辨率(Δt)则由泵浦光(通常为红外光)的脉冲宽度(Δt_{pump})和 XUV 探测光的脉冲宽度($\Delta t_{\mathrm{probe}}$)共同决定[59]:

$$\Delta t=\sqrt{\Delta t_{\mathrm{pump}}^2+\Delta t_{\mathrm{probe}}^2}。\tag{5}$$

XUV 探测光的脉冲宽度受到光源线宽和驱动光的脉冲宽度的限制,并且 XUV 脉冲经过光栅时脉冲前倾会造成进一步的脉冲展宽。光栅带来的脉冲前倾[99]可表示为

$$\Delta\tau\approx\frac{0.5}{c}|m|\lambda' N,\tag{6}$$

式中:$\Delta\tau$为脉冲前倾量;c为光速;λ'为 XUV 波长;N为 XUV 照射到的光栅刻线数。通常为了减小光栅带来的脉冲前倾,需要减小照射到的光栅刻线数。OPM 光栅由于光束传播方向和光栅刻线平行,在掠入射下其照射到的刻线数要比 CDM 光栅小得多,故其脉冲前倾要远小于 CDM 光栅[96,99]。但同时 OPM 光栅的能量分辨能力比不上同刻线密度的 CDM 光栅[99]。延长单色仪臂长有助于获得更高的能量分辨率[100],并使单色仪出口处的 XUV 焦斑直径接近 XUV 产生处的焦斑直径[55]。同时,延长臂长意味着可以使用更小刻线数的光栅实现所需的分光效果,光栅的时间展宽量也会减小。校正单色仪中的球差、慧差和像散需要借助波前探测器对单色仪中的轮胎镜及光栅进行精细调节[101]。

假设 XUV 光脉冲在时域和频域上均为高斯分布,则 XUV 谱线宽度和探测光脉宽能达到的最好理论极限[102-103]为

$$\Delta E_{\mathrm{XUV}}\times\Delta t_{\mathrm{probe}}=1825\ \mathrm{meV\cdot fs}。\tag{7}$$

然而,由于单色仪对脉冲展宽的影响,实际的 Tr-ARPES 很难达到这一理论极限。同时,更窄的谱线宽度或探测光脉宽会对高次谐波的驱动激光提出要求,而驱动激光一般是经过分光后作为泵浦光的,因此会对泵浦光的脉宽产生影响。故本文使用泵浦探测实验装置的能量分辨率与时间分辨率的乘积 $R=\Delta E\times\Delta t$ 作为泵浦探测光源综合性能的衡量指标,部分代表性泵浦探测光源的性能指标如图 3 所示。

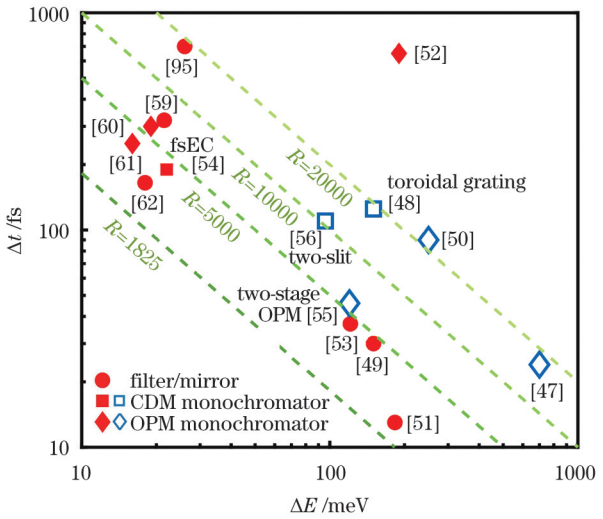

图 3　泵浦探测光源的性能,空心标记表示实验装置的 XUV 线宽由单色仪决定,实心标记表示装置的 XUV 线宽由光源自身决定

Fig. 3　Performances of pump-probe light sources in which hollow marks indicate that XUV linewidth of experimental device is determined by monochromator, and solid marks indicate that XUV linewidth of device is determined by light source itself

侧重于能量分辨的泵浦探测光源,可以清晰地观测到材料的能级细节,但难以捕捉较快的动力学事件,其一般使用金属膜等滤光介质或单色仪选取单阶谐波。在这些设计中,XUV 探测光的线宽不通过单色仪调节,而是直接由高次谐波的光源线宽本身决定。在使用单色仪的设计中,由于此时光栅只需要起到选择单阶谐波的作用,其能量分辨率允许很低,使用刻线密

度较低的OPM光栅即可满足需求，其时间展宽量为50～100 fs[60]。如果进一步忽略XUV光子能量调谐需求，可以用金属膜等代替光栅，达到选出单阶谐波的目的，其时间展宽可以忽略不计。窄线宽的高次谐波光源需要长脉冲的驱动激光产生，而高重复频率、长脉冲的激光峰值功率较低，很难高效率地产生高次谐波，其光子通量一般只在10^8 photon/s量级[59-60,62]。并且，虽然此时XUV光源线宽和脉宽可以接近傅里叶变换极限，但驱动光脉宽很宽，导致较宽的泵浦光脉宽和较差的时间分辨率，使得其综合性能变差。为了提升其综合性能，需要将泵浦飞秒光压缩，这需要驱动激光具有足够高的单脉冲能量，使得其作为高次谐波驱动光后剩余的脉冲能量足够进行非线性压缩，这对激光器提出了较高要求。另一种方案是使用另一台激光器的激光，与驱动激光同步后作为泵浦光[62]，或为泵浦光增加放大模块，这种方法会增加系统的复杂度，但可以有效地提升泵浦探测光源的综合性能。

侧重于时间分辨的泵浦探测光源，可以捕捉极短时间内的动力学过程，但难以分辨具体的能级，一般也是使用金属膜作为单色化器件[49,51,53]。由于高时间分辨率的XUV光本身的光谱较宽，故无需能量分辨能力高的单色仪。同时由于短脉冲XUV光的驱动激光也是短脉冲激光，故其综合时间分辨能力强。而且短脉冲的飞秒激光更容易进行脉冲压缩，泵浦光脉冲压缩后光源的综合性能R甚至可以逼近XUV线宽和脉宽的理论极限1825 meV·fs[51]。

能量分辨能力和时间分辨能力均衡的泵浦探测光源需要短脉冲飞秒激光作为驱动光源以产生短脉冲XUV，但需要同时控制XUV的线宽，因此需要使用单色仪控制能量分辨率。使用单色仪获得较高的能量分辨率，需要光栅有足够高的刻线密度，这同时带来了严重的脉冲前倾。虽然OPM光栅比CDM光栅的脉冲前倾更小，但其仍不能使泵浦探测光源获得较高的综合能力[48,50]，需要进一步减小光栅带来的脉冲前倾。Wang等[56]利用脉冲前倾的空间分布特性，在离焦面增加狭缝以减小脉冲前倾，CDM光栅的脉冲前倾被限制为40 fs，理论结果表明，使用双狭缝结构能够获得比目前可调单狭缝更好的实验结果。Csizmadia等[55]设计了使用两套OPM单色仪的传输方案，第一套单色仪用来调节XUV的线宽，第二套单色仪用来补偿光栅带来的脉冲前倾。这种设计可以几乎完全补偿光栅带来的脉冲前倾，将其控制为4 fs。虽然这两种脉冲前倾控制方案都需要牺牲光子通量，但短脉冲驱动激光容易产生高通量的高次谐波[55-56]，其最高单阶谐波通量甚至可以达到10^{12} photon/s[56]。因此其通量减少是可以接受的，通过控制脉冲前倾有希望获得能量分辨能力和时间分辨能力均衡的高综合性能泵浦探测光源。

影响泵浦探测实验能量分辨率的重要因素还有空间电荷效应[104]，其过程如图4[105]所示。

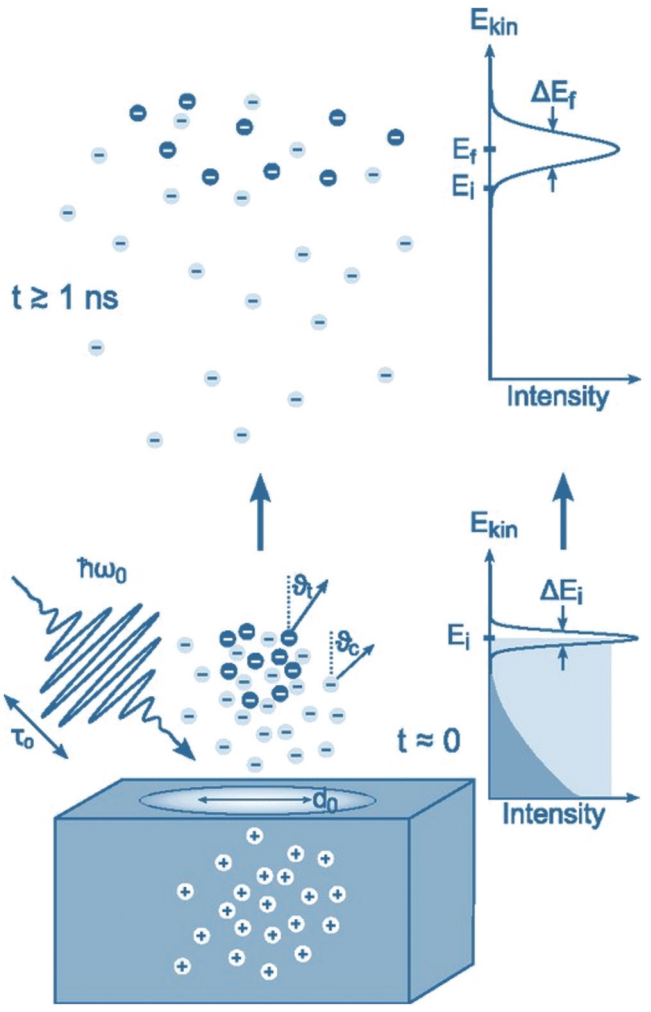

图4 泵浦探测实验中的空间电荷效应[105]

Fig. 4 Space charge effect in pump-probe experiment[105]

当飞秒量级的XUV脉冲聚焦到样品上时，会在极小的空间内产生大量光电子。光电子间的库仑作用会使电子波包变得弥散，造成光电子动能的展宽，能量分辨率变差。同时，样品处残留的正电荷还会对电子波包产生牵引作用，导致能级测量结果的偏移。解决空间电荷效应的基本手段是使用高重复频率的XUV光源，在保持光子通量不变的情况下减少单个XUV脉冲所包含的光子数。然而，即使光源重复频率达到100 kHz以上，也仍然会有足以对实验结果产生明显影响的空间电荷效应[56,59-60]，故需要限制XUV光源的光子通量。目前已有许多研究对空间电荷效应进行了模型推导[104,106-107]，但预测准确度较高的方法还是蒙特卡罗模拟[56,105]。适当增大光斑尺寸也是减小空间电荷效应的有效方法之一[56]，但过大的光斑会带来泵浦探测实验信噪比的下降，因此通常Tr-ARPES样品处的光斑大小都控制在100 μm左右[50,55,60]。

对于以阿秒瞬态吸收光谱为代表的阿秒谱学应用，其泵浦探测实验和Tr-ARPES等飞秒极紫外谱学研究有所不同。在阿秒瞬态吸收光谱中，红外光作为

泵浦光，XUV阿秒脉冲作为探测光。红外电场对气体分子进行调控，此时XUV通过气体分子，其吸收光谱可以反映出能级信息[13]。由于此时泵浦探测是在红外光场和XUV脉冲之间进行的，故其时间分辨率主要取决于XUV的脉冲宽度，可以达到百阿秒量级。阿秒瞬态吸收光谱实验对XUV光谱的细节进行测量，因此其能量分辨率不会受到XUV脉冲宽度的限制，主要取决于光谱仪和探测器。XUV光谱仪通常使用平场光栅光谱仪，对XUV光谱进行分光并将其分布在一定尺寸的XUV探测器上，平场光栅的光谱范围需要覆盖XUV脉冲所测的光谱范围。此时，XUV光谱的分散程度（$\mathrm{d}\lambda/\mathrm{d}x$）表示为光谱宽度（$L$）与探测器直径（$D$）的商。任意XUV探测器都有基本分辨单元的大小限制，例如微通道板（MCP）/磷光屏的基本分辨单元（d）约为25 μm[108]，而X射线相机的d则可以达到13 μm[109]。此时光谱仪的波长分辨率可以粗略表示为$\Delta\lambda_{\mathrm{s}}=d\times L/D$[110]。然而在实际实验中，光谱仪的分辨率由XUV焦斑大小、探测器的空间分辨能力以及可见光电荷耦合器件（CCD）的空间分辨能力共同决定，这些因素极大降低了光谱仪所能达到的分辨极限[111]。特别是XUV探测器和焦平面的微小位移，导致XUV光斑大小发生变化，可见光CCD将大尺寸荧光屏成像到小尺寸探测器上，例如Wang等[10]通过光线追迹计算，得到了10 meV的理论能量分辨率，但由于上述因素，实际分辨率只能达到60 meV。故发展大面阵、高空间分辨率的极紫外探测器是提高阿秒光谱学研究测量精度的重要手段。

6 总结与展望

人们对物理过程的探索及光学应用的发展对极紫外光源提出了其他要求。例如，具有轨道角动量的极紫外光源在超分辨成像和光学传感应用中受到重视[112-115]，目前已经能在实验上得到具有涡旋光场性质的高次谐波[116-121]。而圆偏振高次谐波则在圆二向色性研究中发挥重要作用[122-124]，目前改变XUV偏振状态最常用的方法是借助平面镜的四次反射[125]。在生物成像和纳米显微成像中，极紫外光源在窄线宽的基础上还须具备光谱可调谐特性[126]，目前有多种方法可以实现高次谐波的光谱调谐，如使用光参量放大（OPA）驱动光源和使用长波导气体靶[126-129]。极紫外光学频率梳有望用于下一代“核时钟”的研制[130]以及基本常数变化的探索[131]，也是极紫外光源的重要应用之一[132]。比起飞秒光学频率梳，极紫外光学频率梳由于在光学频率上有数量级的提升，故能够实现更为精确的时间和频率分辨。为了得到极紫外光学频率梳，不仅需要重复频率在1 MHz以上的高重复频率飞秒激光作为高次谐波的驱动源，还需要锁定驱动激光的重复频率和载波包络相移频率[133]，并使用飞秒共振增强腔等技术实现极紫外光梳的耦合输出[134]。这些实验和改进无疑使超快极紫外光源得到了进一步的发展。

目前人们已经对极紫外光源展开了深入的探索，对高次谐波产生以及光源的调控乃至实验束线的分辨率控制进行了充分的研究。极紫外光源的发展使得Tr-ARPES、符合测量、阿秒瞬态吸收光谱和显微成像等得到了快速进步。未来的高重复频率极紫外光源将向更高光子通量以及MHz以上的更高重复频率方向发展，科学家们将追求更高光子能量和更短脉宽的阿秒极紫外光源。对XUV光谱、线宽、脉宽等的操控会催生新的束线设计方案和新的光学元件，这些发展最终会促进基础物理研究和光学的先进应用，从而引领科学与技术的发展进步。

参 考 文 献

[1] McPherson A, Gibson G, Jara H, et al. Studies of multiphoton production of vacuum-ultraviolet radiation in the rare gases[J]. Journal of the Optical Society of America B, 1987, 4(4): 595-601.

[2] Ferray M, L'Huillier A, Li X F, et al. Multiple-harmonic conversion of 1064 nm radiation in rare gases[J]. Journal of Physics B: Atomic Molecular Physics, 1988, 21(3): L31-L35.

[3] Véniard V, Taïeb R, Maquet A. Phase dependence of (N+1)-color (N>1) ir-uv photoionization of atoms with higher harmonics [J]. Physical Review A, 1996, 54(1): 721-728.

[4] Nisoli M, Sansone G. New frontiers in attosecond science[J]. Progress in Quantum Electronics, 2009, 33(1): 17-59.

[5] Itatani J, Levesque J, Zeidler D, et al. Tomographic imaging of molecular orbitals[J]. Nature, 2004, 432(7019): 867-871.

[6] Cavalieri A L, Müller N, Uphues T, et al. Attosecond spectroscopy in condensed matter[J]. Nature, 2007, 449(7165): 1029-1032.

[7] Haarlammert T, Zacharias H. Application of high harmonic radiation in surface science[J]. Current Opinion in Solid State and Materials Science, 2009, 13(1/2): 13-27.

[8] Cheng Y, Chini M, Wang X W, et al. Reconstruction of an excited-state molecular wave packet with attosecond transient absorption spectroscopy[J]. Physical Review A, 2016, 94(2): 023403.

[9] Chen S H, Bell M J, Beck A R, et al. Light-induced states in attosecond transient absorption spectra of laser-dressed helium[J]. Physical Review A, 2012, 86(6): 063408.

[10] Wang X W, Chini M, Cheng Y, et al. In situ calibration of an extreme ultraviolet spectrometer for attosecond transient absorption experiments[J]. Applied Optics, 2013, 52(3): 323-329.

[11] Saito N, Sannohe H, Ishii N, et al. Real-time observation of electronic, vibrational, and rotational dynamics in nitric oxide with attosecond soft X-ray pulses at 400 eV[J]. Optica, 2019, 6(12): 1542-1546.

[12] Saito N, Douguet N, Sannohe H, et al. Attosecond electronic dynamics of core-excited states of N_2O in the soft X-ray region[J]. Physical Review Research, 2021, 3(4): 043222.

[13] Pertot Y, Schmidt C, Matthews M, et al. Time-resolved X-ray absorption spectroscopy with a water window high-harmonic source [J]. Science, 2017, 355(6322): 264-267.

[14] Chew A, Douguet N, Cariker C, et al. Attosecond transient absorption spectrum of argon at the $L_{2,3}$ edge[J]. Physical Review A, 2018, 97(3): 031407.

[15] Buades B, Picón A, Berger E, et al. Attosecond state-resolved carrier motion in quantum materials probed by soft X-ray XANES [J]. Applied Physics Reviews, 2021, 8(1): 011408.

[16] Mikaelsson S, Vogelsang J, Guo C, et al. A high-repetition rate

attosecond light source for time-resolved coincidence spectroscopy [J]. Nanophotonics, 2020, 10(1): 424.

[17] Ravasio A, Gauthier D, Maia F R N C, et al. Single-shot diffractive imaging with a table-top femtosecond soft X-ray laser-harmonics source[J]. Physical Review Letters, 2009, 103(2): 028104.

[18] Vu Le H, Ba Dinh K, Hannaford P, et al. High resolution coherent diffractive imaging with a table-top extreme ultraviolet source[J]. Journal of Applied Physics, 2014, 116(17): 173104.

[19] Rupp D, Monserud N, Langbehn B, et al. Coherent diffractive imaging of single helium nanodroplets with a high harmonic generation source[J]. Nature Communications, 2017, 8(1): 493.

[20] Zürch M, Rothhardt J, Hädrich S, et al. Real-time and sub-wavelength ultrafast coherent diffraction imaging in the extreme ultraviolet[J]. Scientific Reports, 2014, 4: 7356.

[21] Huijts J, Fernandez S, Gauthier D, et al. Broadband coherent diffractive imaging[J]. Nature Photonics, 2020, 14: 618-622.

[22] Chen F M, Wang J, Pan M J, et al. Time-resolved ARPES with tunable 12–21.6 eV XUV at 400 kHz repetition rate[J]. Review of Scientific Instruments, 2023, 94(4): 043905.

[23] Carpene E, Mancini E, Dallera C, et al. A versatile apparatus for time-resolved photoemission spectroscopy via femtosecond pump-probe experiments[J]. The Review of Scientific Instruments, 2009, 80(5): 055101.

[24] Smallwood C L, Jozwiak C, Zhang W T, et al. An ultrafast angle-resolved photoemission apparatus for measuring complex materials [J]. The Review of Scientific Instruments, 2012, 83(12): 123904.

[25] Boschini F, Hedayat H, Dallera C, et al. An innovative Yb-based ultrafast deep ultraviolet source for time-resolved photoemission experiments[J]. The Review of Scientific Instruments, 2014, 85 (12): 123903.

[26] Yan C H, Green E, Fukumori R, et al. An integrated quantum material testbed with multi-resolution photoemission spectroscopy [J]. Review of Scientific Instruments, 2021, 92(11): 113907.

[27] Karni O, Barré E, Pareek V, et al. Structure of the Moiré exciton captured by imaging its electron and hole[J]. Nature, 2022, 603 (7900): 247-252.

[28] Zhou X J, He S L, Liu G D, et al. New developments in laser-based photoemission spectroscopy and its scientific applications: a key issues review[J]. Reports on Progress in Physics, 2018, 81(6): 062101.

[29] Corkum P B. Plasma perspective on strong field multiphoton ionization[J]. Physical Review Letters, 1993, 71(13): 1994-1997.

[30] Klaiber M, Hatsagortsyan K Z, Keitel C H. Fully relativistic laser-induced ionization and recollision processes[J]. Physical Review A, 2007, 75(6): 063413.

[31] Strickland D, Mourou G. Compression of amplified chirped optical pulses[J]. Optics Communications, 1985, 56(3): 219-221.

[32] 赵昆. 激光、啁啾脉冲放大、超快光学和诺贝尔奖[J]. 科学通报, 2019, 64(14): 1433-1440.
Zhao K. Laser, chirped pulse amplification, ultrafast optics, and Nobel Prize in Physics[J]. Chinese Science Bulletin, 2019, 64(14): 1433-1440.

[33] 王阁阳, 吕仁冲, 许思源, 等. 高重复频率高次谐波驱动源技术[J]. 科学通报, 2021, 66(8): 924-939.
Wang G Y, Lü R C, Xu S Y, et al. High repetition rate ultrafast laser technology for driving high-order harmonic generation[J]. Chinese Science Bulletin, 2021, 66(8): 924-939.

[34] Schmidt J, Guggenmos A, Chew S H, et al. Development of a 10 kHz high harmonic source up to 140 eV photon energy for ultrafast time-, angle-, and phase-resolved photoelectron emission spectroscopy on solid targets[J]. The Review of Scientific Instruments, 2017, 88(8): 083105.

[35] Chiang C T, Blättermann A, Huth M, et al. High-order harmonic generation at 4 MHz as a light source for time-of-flight photoemission spectroscopy[J]. Applied Physics Letters, 2012, 101(7): 071116.

[36] Heyl C M, Güdde J, L'Huillier A, et al. High-order harmonic generation with μJ laser pulses at high repetition rates[J]. Journal of Physics B: Atomic, Molecular and Optical Physics, 2012, 45(7): 074020.

[37] Mourou G, Brocklesby B, Tajima T, et al. The future is fibre accelerators[J]. Nature Photonics, 2013, 7: 258-261.

[38] Chang W Z, Zhou T, Siiman L A, et al. Femtosecond pulse spectral synthesis in coherently-spectrally combined multi-channel fiber chirped pulse amplifiers[J]. Optics Express, 2013, 21(3): 3897-3910.

[39] Hädrich S, Demmler S, Rothhardt J, et al. High-repetition-rate sub-5-fs pulses with 12 GW peak power from fiber-amplifier-pumped optical parametric chirped-pulse amplification[J]. Optics Letters, 2011, 36(3): 313-315.

[40] Hädrich S, Klenke A, Hoffmann A, et al. Nonlinear compression to sub-30-fs, 0.5 mJ pulses at 135 W of average power[J]. Optics Letters, 2013, 38(19): 3866-3869.

[41] Jauregui C, Limpert J, Tünnermann A. High-power fibre lasers [J]. Nature Photonics, 2013, 7: 861-867.

[42] Rothhardt J, Hädrich S, Klenke A, et al. 53 W average power few-cycle fiber laser system generating soft x rays up to the water window[J]. Optics Letters, 2014, 39(17): 5224-5227.

[43] Hädrich S, Klenke A, Rothhardt J, et al. High photon flux table-top coherent extreme-ultraviolet source[J]. Nature Photonics, 2014, 8: 779-783.

[44] Hädrich S, Krebs M, Hoffmann A, et al. Exploring new avenues in high repetition rate table-top coherent extreme ultraviolet sources [J]. Light: Science & Applications, 2015, 4(8): e320.

[45] Müller M, Kienel M, Klenke A, et al. 1 kW 1 mJ eight-channel ultrafast fiber laser[J]. Optics Letters, 2016, 41(15): 3439-3442.

[46] Müller M, Aleshire C, Klenke A, et al. 10.4 kW coherently combined ultrafast fiber laser[J]. Optics Letters, 2020, 45(11): 3083-3086.

[47] Frassetto F, Cacho C, Froud C A, et al. Single-grating monochromator for extreme-ultraviolet ultrashort pulses[J]. Optics Express, 2011, 19(20): 19169-19181.

[48] Frietsch B, Carley R, Döbrich K, et al. A high-order harmonic generation apparatus for time- and angle-resolved photoelectron spectroscopy[J]. The Review of Scientific Instruments, 2013, 84 (7): 075106.

[49] Eich S, Stange A, Carr A V, et al. Time- and angle-resolved photoemission spectroscopy with optimized high-harmonic pulses using frequency-doubled Ti: Sapphire lasers[J]. Journal of Electron Spectroscopy and Related Phenomena, 2014, 195: 231-236.

[50] Ojeda J, Arrell C A, Grilj J, et al. Harmonium: a pulse preserving source of monochromatic extreme ultraviolet (30-110 eV) radiation for ultrafast photoelectron spectroscopy of liquids[J]. Structural Dynamics, 2015, 3(2): 023602.

[51] Rohde G, Hendel A, Stange A, et al. Time-resolved ARPES with sub-15 fs temporal and near Fourier-limited spectral resolution [J]. Review of Scientific Instruments, 2016, 87(10): 103102.

[52] Nie Z H, Turcu I C E, Li Y, et al. Spin-ARPES EUV beamline for ultrafast materials research and development[J]. Applied Sciences, 2019, 9(3): 370.

[53] Puppin M, Deng Y, Nicholson C W, et al. Time- and angle-resolved photoemission spectroscopy of solids in the extreme ultraviolet at 500 kHz repetition rate[J]. The Review of Scientific Instruments, 2019, 90(2): 023104.

[54] Mills A K, Zhdanovich S, Na M X, et al. Cavity-enhanced high harmonic generation for extreme ultraviolet time- and angle-resolved photoemission spectroscopy[J]. The Review of Scientific Instruments, 2019, 90(8): 083001.

[55] Csizmadia T, Filus Z, Grősz T, et al. Spectrally tunable ultrashort monochromatized extreme ultraviolet pulses at 100 kHz [J]. APL Photonics, 2023, 8(5): 056105.

[56] Wang J, Chen F M, Pan M J, et al. High-flux wavelength tunable XUV source in the 12 – 40.8 eV photon energy range with

adjustable energy and time resolution for Tr-ARPES applications [J]. Optics Express, 2023, 31(6): 9854-9871.

[57] Lorek E, Larsen E W, Heyl C M, et al. High-order harmonic generation using a high-repetition-rate turnkey laser[J]. The Review of Scientific Instruments, 2014, 85(12): 123106.

[58] Emaury F, Diebold A, Saraceno C J, et al. Compact extreme ultraviolet source at megahertz pulse repetition rate with a low-noise ultrafast thin-disk laser oscillator[J]. Optica, 2015, 2(11): 980-984.

[59] Liu Y Y, Beetar J E, Hosen M M, et al. Extreme ultraviolet time- and angle-resolved photoemission setup with 21.5 meV resolution using high-order harmonic generation from a turn-key Yb: KGW amplifier[J]. The Review of Scientific Instruments, 2020, 91(1): 013102.

[60] Cucini R, Pincelli T, Panaccione G, et al. Coherent narrowband light source for ultrafast photoelectron spectroscopy in the 17-31 eV photon energy range[J]. Structural Dynamics, 2020, 7(1): 014303.

[61] Lee C M, Rohwer T, Sie E J, et al. High resolution time- and angle-resolved photoemission spectroscopy with 11 eV laser pulses [J]. The Review of Scientific Instruments, 2020, 91(4): 043102.

[62] Guo Q D, Dendzik M, Grubišić-Čabo A, et al. A narrow bandwidth extreme ultra-violet light source for time- and angle-resolved photoemission spectroscopy[J]. Structural Dynamics, 2022, 9(2): 024304.

[63] 刘军, 曾志男, 梁晓燕, 等. 超快超强激光及其科学应用发展趋势研究[J]. 中国工程科学, 2020, 22(3): 42-48.
Liu J, Zeng Z N, Liang X Y, et al. Development trend of ultrafast and ultraintense lasers and their scientific application[J]. Strategic Study of CAE, 2020, 22(3): 42-48.

[64] Krebs M, Hädrich S, Demmler S, et al. Towards isolated attosecond pulses at megahertz repetition rates[J]. Nature Photonics, 2013, 7: 555-559.

[65] Furch F J, Witting T, Giree A, et al. CEP-stable few-cycle pulses with more than 190 μJ of energy at 100 kHz from a noncollinear optical parametric amplifier[J]. Optics Letters, 2017, 42(13): 2495-2498.

[66] Witting T, Furch F, Osolodkov M, et al. Generation and characterization of isolated attosecond pulses for coincidence spectroscopy at 100 kHz repetition rate[J]. Journal of Physics: Conference Series, 2020, 1412(7): 072031.

[67] Witting T, Osolodkov M, Schell F, et al. Generation and characterization of isolated attosecond pulses at 100 kHz repetition rate[J]. Optica, 2022, 9(2): 145-151.

[68] Harth A, Guo C, Cheng Y C, et al. Compact 200 kHz HHG source driven by a few-cycle OPCPA[J]. Journal of Optics, 2018, 20(1): 014007.

[69] Guo C, Harth A, Carlström S, et al. Phase control of attosecond pulses in a train[J]. Journal of Physics B: Atomic, Molecular and Optical Physics, 2018, 51(3): 034006.

[70] Cheng Y C, Mikaelsson S, Nandi S, et al. Controlling photoionization using attosecond time-slit interferences[J]. Proceedings of the National Academy of Sciences of the United States of America, 2020, 117(20): 10727-10732.

[71] Borzsonyi A, Cormier E, Lopez-Martens R, et al. Latest progress on the few-cycle, high average power lasers of ELI-ALPS[C]// Ultrafast Optics 2023, March 26-31, 2023, Bariloche, Río Negro, Argentina. Washington, DC: Optica Publishing Group, 2023: M4.1.

[72] 魏志义, 钟诗阳, 贺新奎, 等. 阿秒光学进展及发展趋势[J]. 中国激光, 2021, 48(5): 0501001.
Wei Z Y, Zhong S Y, He X K, et al. Progresses and trends in attosecond optics[J]. Chinese Journal of Lasers, 2021, 48(5): 0501001.

[73] Wernet P, Gaudin J, Godehusen K, et al. Femtosecond time-resolved photoelectron spectroscopy with a vacuum-ultraviolet photon source based on laser high-order harmonic generation[J]. The Review of Scientific Instruments, 2011, 82(6): 063114.

[74] Niu Y, Liu F Y, Liu Y, et al. Pressure-dependent phase matching for high harmonic generation of Ar and N_2 in the tight focusing regime[J]. Optics Communications, 2017, 397: 118-121.

[75] Rothhardt J, Krebs M, Hädrich S, et al. Absorption-limited and phase-matched high harmonic generation in the tight focusing regime[J]. New Journal of Physics, 2014, 16(3): 033022.

[76] Colosimo P, Doumy G, Blaga C I, et al. Scaling strong-field interactions towards the classical limit[J]. Nature Physics, 2008, 4: 386-389.

[77] Lewenstein M, Salières P, L'Huillier A. Phase of the atomic polarization in high-order harmonic generation[J]. Physical Review A, 1995, 52(6): 4747-4754.

[78] Popmintchev T, Chen M C, Bahabad A, et al. Phase matching of high harmonic generation in the soft and hard X-ray regions of the spectrum[J]. Proceedings of the National Academy of Sciences of the United States of America, 2009, 106(26): 10516-10521.

[79] Paul A, Gibson E A, Zhang X S, et al. Phase-matching techniques for coherent soft X-ray generation[J]. IEEE Journal of Quantum Electronics, 2006, 42(1): 14-26.

[80] Filus Z, Ye P, Csizmadia T, et al. Liquid-cooled modular gas cell system for high-order harmonic generation using high average power laser systems[J]. The Review of Scientific Instruments, 2022, 93(7): 073002.

[81] Kim S, Jin J, Kim Y J, et al. High-harmonic generation by resonant plasmon field enhancement[J]. Nature, 2008, 453(7196): 757-760.

[82] Han S, Kim H, Kim Y W, et al. High-harmonic generation by field enhanced femtosecond pulses in metal-sapphire nanostructure [J]. Nature Communications, 2016, 7: 13105.

[83] Zhao J F, Ou H W, Wu G, et al. Evolution of the electronic structure of 1T-$Cu_x TiSe_2$[J]. Physical Review Letters, 2007, 99(14): 146401.

[84] Liu G D, Wang G L, Zhu Y, et al. Development of a vacuum ultraviolet laser-based angle-resolved photoemission system with a superhigh energy resolution better than 1 meV[J]. The Review of Scientific Instruments, 2008, 79(2): 023105.

[85] Jiang J, Liu Z K, Sun Y, et al. Signature of type-II Weyl semimetal phase in $MoTe_2$[J]. Nature Communications, 2017, 8: 13973.

[86] Mandal P S, Springholz G, Volobuev V V, et al. Topological quantum phase transition from mirror to time reversal symmetry protected topological insulator[J]. Nature Communications, 2017, 8(1): 968.

[87] Zhang Y, Wang C L, Yu L, et al. Electronic evidence of temperature-induced Lifshitz transition and topological nature in $ZrTe_5$[J]. Nature Communications, 2017, 8: 15512.

[88] Czerny M, Turner A F. Über den astigmatismus bei spiegelspektrometern[J]. Zeitschrift Für Physik, 1930, 61(11): 792-797.

[89] Guo Q D, Dendzik M, Berntsen M H, et al. Efficient low-density grating setup for monochromatization of XUV ultrafast light sources [J]. Optics Express, 2023, 31(5): 8914-8926.

[90] Loriot V, Quintard L, Karras G, et al. Time-resolved and spectrally resolved ionization with a single ultrashort XUV-IR beamline[J]. Journal of the Optical Society of America B, 2018, 35(4): A67-A74.

[91] Poletto L, Tondello G, Villoresi P. Optical design of a spectrometer-monochromator for the extreme-ultraviolet and soft-X-ray emission of high-order harmonics[J]. Applied Optics, 2003, 42(31): 6367-6373.

[92] Suzuki C, Koike F, Murakami I, et al. Temperature dependent EUV spectra of Gd, Tb and Dy ions observed in the Large Helical Device[J]. Journal of Physics B: Atomic, Molecular and Optical Physics, 2015, 48(14): 144012.

[93] Xu Z, Zhang L, Cheng Y X, et al. An extreme ultraviolet spectrometer working at 10–130 Å for tungsten spectra observation

with high spectral resolution and fast-time response in Experimental Advanced Superconducting Tokamak[J]. Nuclear Instruments and Methods in Physics Research Section A: Accelerators, Spectrometers, Detectors and Associated Equipment, 2021, 1010: 165545.

[94] Nakano N, Kuroda H, Kita T, et al. Development of a flat-field grazing-incidence XUV spectrometer and its application in picosecond XUV spectroscopy[J]. Applied Optics, 1984, 23(14): 2386-2392.

[95] Peli S, Puntel D, Kopic D, et al. Time-resolved VUV ARPES at 10.8 eV photon energy and MHz repetition rate[J]. Journal of Electron Spectroscopy and Related Phenomena, 2020, 243: 146978.

[96] Poletto L, Frassetto F. Time-preserving grating monochromators for ultrafast extreme-ultraviolet pulses[J]. Applied Optics, 2010, 49(28): 5465-5473.

[97] Poletto L, Miotti P, Frassetto F, et al. Double-configuration grating monochromator for extreme-ultraviolet ultrafast pulses[J]. Applied Optics, 2014, 53(26): 5879-5888.

[98] Grazioli C, Callegari C, Ciavardini A, et al. CITIUS: an infrared-extreme ultraviolet light source for fundamental and applied ultrafast science[J]. The Review of Scientific Instruments, 2014, 85(2): 023104.

[99] Poletto L, Frassetto F. Single-grating monochromators for extreme-ultraviolet ultrashort pulses[J]. Applied Sciences, 2012, 3(1): 1-13.

[100] Shvyd'ko Y. Enhanced X-ray angular dispersion and X-ray spectrographs with resolving power beyond 10^8[J]. Proceedings of SPIE, 2012, 8502: 85020J.

[101] Biednov M, Brenner G, Dicke B, et al. Alignment of the aberration-free XUV Raman spectrometer at FLASH[J]. Journal of Synchrotron Radiation, 2019, 26(1): 18-27.

[102] Koch T L, Bowers J E. Nature of wavelength chirping in directly modulated semiconductor lasers[J]. Electronics Letters, 1984, 20(25/26): 1038-1040.

[103] Huang C Z, Duan S F, Zhang W T. High-resolution time- and angle-resolved photoemission studies on quantum materials[J]. Quantum Frontiers, 2022, 1(1): 15.

[104] Al-Obaidi R, Wilke M, Borgwardt M, et al. Ultrafast photoelectron spectroscopy of solutions: space-charge effect[J]. New Journal of Physics, 2015, 17(9): 093016.

[105] Hellmann S, Rossnagel K, Marczynski-Bühlow M, et al. Vacuum space-charge effects in solid-state photoemission[J]. Physical Review B, 2009, 79(3): 035402.

[106] Long J P, Itchkawitz B S, Kabler M N. Photoelectron spectroscopy of laser-excited surfaces by synchrotron radiation[J]. Journal of the Optical Society of America B: Optical Physics, 1996, 13(1): 201-208.

[107] Siwick B J, Dwyer J R, Jordan R E, et al. Ultrafast electron optics: propagation dynamics of femtosecond electron packets[J]. Journal of Applied Physics, 2002, 92(3): 1643-1648.

[108] Vallerga J V, Siegmund O H W. 2K×2K resolution element photon counting MCP sensor with >200 kHz event rate capability[J]. Nuclear Instruments and Methods in Physics Research Section A: Accelerators, Spectrometers, Detectors and Associated Equipment, 2000, 442(1/2/3): 159-163.

[109] Hague C F, Underwood J H, Avila A, et al. Plane-grating flat-field soft X-ray spectrometer[J]. Review of Scientific Instruments, 2005, 76(2): 023110.

[110] Schwanda W, Eidmann K, Richardson M C. Characterization of a flat-field grazing-incidence XUV spectrometer[J]. Journal of X-Ray Science and Technology, 1993, 4(1): 8-17.

[111] Chini M, Wang H, Zhao B Z, et al. Attosecond absorption spectroscopy[M]//Yamnouchi K, Midorikawa K. Progress in ultrafast intense laser science. Springer series in chemical physics. Heidelberg: Springer, 2013, 104: 135-150.

[112] Betzig E, Patterson G H, Sougrat R, et al. Imaging intracellular fluorescent proteins at nanometer resolution[J]. Science, 2006, 313(5793): 1642-1645.

[113] Torres J P, Torner L. Twisted photons applications of light with orbital angular momentum[M]. Weinheim: Wiley-VCH Verlag, 2011.

[114] Willner A E, Huang H, Yan Y, et al. Optical communications using orbital angular momentum beams[J]. Advances in Optics and Photonics, 2015, 7(1): 66-106.

[115] Wang B, Tanksalvala M, Zhang Z, et al. Coherent Fourier scatterometry using orbital angular momentum beams for defect detection[J]. Optics Express, 2021, 29(3): 3342-3358.

[116] Hernández-García C, Picón A, San Román J, et al. Attosecond extreme ultraviolet vortices from high-order harmonic generation[J]. Physical Review Letters, 2013, 111(8): 083602.

[117] Gariepy G, Leach J, Kim K T, et al. Creating high-harmonic beams with controlled orbital angular momentum[J]. Physical Review Letters, 2014, 113(15): 153901.

[118] Géneaux R, Camper A, Auguste T, et al. Synthesis and characterization of attosecond light vortices in the extreme ultraviolet[J]. Nature Communications, 2016, 7: 12583.

[119] Dorney K M, Rego L, Brooks N J, et al. Controlling the polarization and vortex charge of attosecond high-harmonic beams via simultaneous spin-orbit momentum conservation[J]. Nature Photonics, 2019, 13: 123-130.

[120] Paufler W, Böning B, Fritzsche S. High harmonic generation with Laguerre-Gaussian beams[J]. Journal of Optics, 2019, 21(9): 094001.

[121] Rego L, Dorney K M, Brooks N J, et al. Generation of extreme-ultraviolet beams with time-varying orbital angular momentum[J]. Science, 2019, 364(6447): eaaw9486.

[122] Cho S, Park J H, Hong J, et al. Experimental observation of hidden berry curvature in inversion-symmetric bulk 2*H*-WSe_2[J]. Physical Review Letters, 2018, 121(18): 186401.

[123] Cho S, Park J H, Huh S, et al. Studying local Berry curvature in 2H-WSe_2 by circular dichroism photoemission utilizing crystal mirror plane[J]. Scientific Reports, 2021, 11(1): 1684.

[124] Schüler M, De Giovannini U, Hübener H, et al. Local Berry curvature signatures in dichroic angle-resolved photoelectron spectroscopy from two-dimensional materials[J]. Science Advances, 2020, 6(9): eaay2730.

[125] Comby A, Rajak D, Descamps D, et al. Ultrafast polarization-tunable monochromatic extreme ultraviolet source at high-repetition-rate[J]. Journal of Optics, 2022, 24(8): 084003.

[126] Yao J P, Cheng Y, Chen J, et al. Generation of narrow-bandwidth, tunable, coherent xuv radiation using high-order harmonic generation[J]. Physical Review A, 2011, 83(3): 033835.

[127] Seres J, Seres E, Serrat C, et al. Spectral shift and split of harmonic lines in propagation affected high harmonic generation in a long-interaction gas tube[J]. Atoms, 2023, 11(12): 150.

[128] Shan B, Cavalieri A, Chang Z. Tunable high harmonic generation with an optical parametric amplifier[J]. Applied Physics B, 2002, 74(1): s23-s26.

[129] Tani F, Frosz M H, Travers J C, et al. Continuously wavelength-tunable high harmonic generation via soliton dynamics[J]. Optics Letters, 2017, 42(9): 1768-1771.

[130] Campbell C J, Radnaev A G, Kuzmich A. Wigner crystals of ^{229}Th for optical excitation of the nuclear isomer[J]. Physical Review Letters, 2011, 106(22): 223001.

[131] Berengut J C, Dzuba V A, Flambaum V V, et al. Electron-hole transitions in multiply charged ions for precision laser spectroscopy and searching for variations in α[J]. Physical Review Letters, 2011, 106(21): 210802.

[132] 郑立, 刘寒, 汪会波, 等. 极紫外飞秒光学频率梳的产生与研究进展[J]. 物理学报, 2020, 69(22): 224203.
Zheng L, Liu H, Wang H B, et al. Generation and research progress of femtosecond optical frequency combs in extreme ultraviolet[J]. Acta Physica Sinica, 2020, 69(22): 224203.

[133] Jones R J, Thomann I, Ye J. Precision stabilization of

femtosecond lasers to high-finesse optical cavities[J]. Physical Review A, 2004, 69(5): 051803.

[134] Jones R J, Moll K D, Thorpe M J, et al. Phase-coherent frequency combs in the vacuum ultraviolet via high-harmonic generation inside a femtosecond enhancement cavity[J]. Physical Review Letters, 2005, 94(19): 193201.

Research Progress in Generation and Spectral Technology of High-Repetition-Rate Extreme-Ultraviolet-Light Sources

Wang Ji[1,2], Zhao Kun[1,2*]

[1]*Beijing National Laboratory for Condensed Matter Physics, Institute of Physics, Chinese Academy of Sciences, Beijing* 100190, *China*;

[2]*Songshan Lake Materials Laboratory, Dongguan* 523808, *Guangdong, China*

Abstract

Significance The extreme-ultraviolet high-harmonic light source has attracted significant attention in electron dynamics because of its strong coherence, short pulse duration, and high photon energy. It has been applied in various spectroscopy and imaging studies. Using a high repetition rate, high photon flux, narrow linewidth, femtosecond extreme-ultraviolet-light source (1 fs=10^{-15} s) enables direct observation of conduction band structures and femtosecond-scale electron dynamics in materials. Furthermore, processes such as electron tunneling and molecular dissociation can be investigated extensively using a broadband attosecond light source. In recent years, the development of water window spectral-range wide-spectrum attosecond light sources has facilitated the detection of reaction pathways between molecules and the motion of charge carriers on material surfaces. By applying electron and ion detection techniques, time-resolved coherent measurements and other attosecond transient spectroscopy studies have been conducted. For attosecond-scale electron spectroscopy measurements, the number of events in a single-shot measurement is often insufficient, making low-repetition-rate light sources inadequate for obtaining reliable statistical data. Therefore, it is necessary to use high-repetition-rate extreme-ultraviolet-light sources.

The efficiency and photon number per pulse of high-repetition-rate high-harmonic generation are significantly lower than those of low-repetition-rate high-harmonic generation. The single-pulse energy of high-repetition-rate driving lasers is lower than that of low-repetition-rate driving lasers; therefore, tight focusing is required to achieve the high-intensity field necessary for high harmonic generation. However, the interaction region of the laser and gas is small during tight focusing, making it relatively difficult to achieve the required phase-matching conditions. Consequently, the conversion efficiency of high-repetition-rate high-harmonic generation is low. Various methods have been developed in terms of driving laser, high-harmonic-generation methods, and beamline design to improve the photon flux of high-repetition-rate high-harmonic generation.

The use of extreme-ultraviolet high-harmonic light sources during experiments requires the presence of a monochromator or spectrometer. A spectrometer with high acquisition efficiency and high resolution is required to optimize high harmonic generation by adjusting the interaction configuration and characterize energy level transitions using attosecond transient absorption spectroscopy. In pump-probe experiments for dynamics research, a femtosecond extreme-ultraviolet-light source with good energy and time resolutions is required. A monochromator is required to select individual orders of high harmonics, achieving energy resolution control and minimizing the time broadening caused by the monochromator. Significant efforts have been made in beamline design to use extreme-ultraviolet high-harmonic-light sources in physics experiments.

Progress Currently, extreme-ultraviolet high-harmonic light sources are advancing towards higher photon fluxes and repetition rates, which places higher demands on the repetition rate and single-pulse energy of femtosecond lasers. Chiang *et al*. used a long-cavity titanium sapphire laser to increase the repetition rate of the driving laser to 4 MHz and achieved high harmonic output. In 2015, Hädrich *et al*. used a fiber laser to increase the repetition rate of high harmonics to 10.7 MHz. The highest average power of femtosecond lasers has now exceeded 10 kW.

The generation and optimization of high harmonics have been ongoing research topics. Using high-performance and high-repetition-rate lasers with high energy and few-cycle pulse length can prevent tight focusing and achieve high harmonic generation efficiency using fundamental-frequency-driving light. Csizmadia et *al*. directly generated high harmonics using a few-cycle 1030 nm driver laser with a repetition rate of 100 kHz and obtained a high-photon-flux extreme-ultraviolet-light source. By applying pulse compression, shorter pulse high-repetition-rate driving light can more easily achieve the peak power density required for high harmonic generation, thus achieving higher efficiency than long-pulse driving light. Wang *et al*. applied dual-color field-assisted pulse compression to obtain a high-photon-flux extreme-ultraviolet-light source. High-repetition-rate high-harmonic light sources above the MHz level require field-enhanced methods for generation. Among them, resonant enhancement cavities have been applied to time- and angle-resolved photoemission spectroscopy (Tr-ARPES) beamlines. Mills *et al*. used a fiber laser with a repetition rate of 60 MHz to obtain a high-photon-flux extreme ultraviolet-light source.

Monochromators and spectrometers are essential instruments for applying extreme ultraviolet-light sources. Rohde *et al*. used a metal film as a monochromatizing device while compressing the pump light, and the comprehensive performance of the compressed light source can approach the Fourier transform limit of extreme ultraviolet (XUV). Wang *et al*. developed an approach to reduce the pulse front tilt by adding slits at the defocused plane, taking advantage of the spatial distribution characteristics of forward-tilted pulses. Csizmadia *et al*. designed a transmission scheme using two off-plane mount (OPM) monochromators, with the first monochromator used to adjust the line width of XUV and the second monochromator used to compensate for the pulse front tilt generated by the grating. This design is used to almost completely compensate for the pulse front tilt generated by the grating.

Conclusions and Prospects High-repetition-rate extreme-ultraviolet-light sources have been widely used in electron dynamics research and have potential for applications in attosecond spectroscopy and microscopic imaging. These light sources are evolving towards increased repetition rates, photon fluxes, photon energies, and decreased pulse durations. This review summarizes the generation and control of high-repetition-rate extreme-ultraviolet-light sources and the optimization of their resolving capability for applications. Future development trends of such light sources are also discussed.

Key words nonlinear optics; ultrafast optics; high harmonic generation; extreme ultraviolet light source